

## Structure analysis of CoPt alloy film with metastable ordered phases of $L1_1$ and $B_h$ formed on Ru(0001) underlayer

Mitsuru Ohtake<sup>1,a</sup>, Daisuke Suzuki<sup>1</sup>, Fumiyoshi Kirino<sup>2</sup>, and Masaaki Futamoto<sup>1</sup>

<sup>1</sup>Faculty of Science and Engineering, Chuo University, 1-13-27 Kasuga, Bunkyo-ku, Tokyo 112-8551, Japan

<sup>2</sup>Graduate School of Fine Arts, Tokyo University of the Arts, 12-8 Ueno-koen, Taito-ku, Tokyo 110-8714, Japan

**Abstract.** CoPt alloy films of 40 nm thickness are prepared on MgO(111) substrates with and without Ru(0001) underlayer at 300 °C by radio-frequency magnetron sputtering. CoPt films with the close-packed plane parallel to the substrate surface grow epitaxially on the Ru underlayer as well as on the MgO substrate. Flat surfaces with the arithmetical mean roughness value of 0.2 nm are realized for both films. The crystal structure is determined by considering the atomic stacking sequence of close-packed plane and the order degree. The film formed on MgO substrate consists of an fcc-based  $L1_1$  ordered crystal, whereas the film grown on Ru underlayer involves an hcp-based  $B_h$  ordered crystal in addition to the  $L1_1$  ordered crystal. The order degrees of films formed on MgO substrate and Ru underlayer are 0.30 and 0.34, respectively. The  $L1_1$  crystal consists of two variants whose stacking sequences of close-packed plane are ABCABC... and ACBACB..., while the  $B_h$  crystal is a single-crystal with the stacking sequence of ABAB... Formation of  $B_h$  crystal is promoted on the Ru underlayer. The film formed on Ru underlayer shows a strong perpendicular magnetic anisotropy reflecting the magnetocrystalline anisotropies of  $L1_1$  and  $B_h$  crystals.

### 1 Introduction

Magnetic thin films with the uniaxial magnetocrystalline anisotropy energy ( $K_u$ ) greater than  $10^7$  erg/cm<sup>3</sup> and the easy magnetization axis perpendicular to the substrate surface have been investigated for applications such as recording media and magnetoresistive random access memory devices, etc. CoPt or FePt alloy around the equiatomic composition has an ordered phase of  $L1_0$ . CoPt and FePt bulk crystals with  $L1_0$  structure show  $K_u$  of  $4.9 \times 10^7$  [1] and  $6.6 \times 10^7$  [2] erg/cm<sup>3</sup>, respectively. In order to prepare a CoPt or an FePt film with high  $K_u$  value, a high degree of  $L1_0$  ordering, which is realized by employing high-temperature processing around 600 °C, is necessary. However, film deposition at an elevated temperature enhances the film surface roughness [3]. Surface flatness is an important technological issue for practical applications. High  $K_u$  film materials which can be prepared at moderate temperatures are required.

Formation of metastable  $L1_1$  ordered phase has been recognized for CoPt alloy films deposited on MgO(111) substrates around 300 °C [4–8]. The  $L1_1$  structure consists of alternate stacking of close-packed planes of Co and Pt, as shown in figure 1(a). In the present paper, the fcc-based notations of plane and direction are applied to the  $L1_1$  and the  $L1_0$  structures for simple comparison with the disordered  $A1$  structure, though the accurate structures are rhombohedral and tetragonal, respectively. Furthermore, the unit cell shown in figure 1(a) is used for

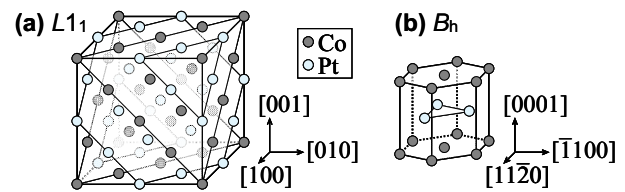
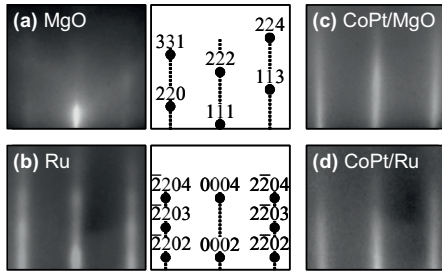


Fig. 1. Crystal structures of (a)  $L1_1$  and (b)  $B_h$ .

the fcc-based structures. An  $L1_1$  CoPt film with the long-range order degree ( $S$ ) of 0.33 is reported to show  $K_u$  of  $1.7 \times 10^7$  erg/cm<sup>3</sup> along the direction normal to the close-packed plane [5]. A theoretical calculation suggests that the  $K_u$  value increases up to  $10^8$  erg/cm<sup>3</sup> with increasing the  $S$  value [9]. Therefore, the  $L1_1$  ordered CoPt alloy is one of the strong candidates for a high  $K_u$  material which can be applicable to future magnetic thin film devices.

The fcc- and the hcp-based structures respectively consist of atomic stacking sequences of ABCABC... and ABAB... along the direction normal to the close-packed plane. The crystal structure is known to easily vary between the two structures through introduction of stacking faults parallel to the close-packed plane. There is thus a possibility that an hcp-based ordered phase of  $B_h$  shown in figure 1(b) is formed in CoPt films. However, there are few reports on the structural analysis of films including ordered phases by taking into account the stacking sequence of close-packed plane [7, 8, 10]. The stacking sequence of Co-based alloy film is influenced by

<sup>a</sup> Corresponding author: ohtake@futamoto.elect.chuo-u.ac.jp



**Fig. 2.** (a, b) RHEED patterns and the schematic diagrams of (a) an MgO(111) substrate and (b) an Ru underlayer deposited on MgO substrate. (c, d) RHEED patterns observed for CoPt films deposited on (c) MgO substrate and (d) Ru underlayer. The incident electron beam is parallel to MgO[1 $\bar{1}$ 0].

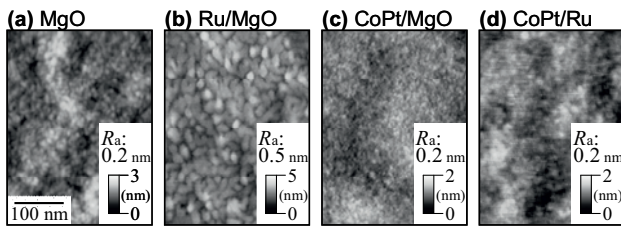


**Fig. 3.** AFM images observed for (a) an MgO(111) substrate, (b) an Ru(0001) underlayer deposited on MgO substrate, and (c, d) CoPt films deposited on (c) MgO substrate and (d) Ru underlayer.

the substrate or underlayer material [11]. Ru has been used as an underlayer to prepare Co-Pt-Cr films with hcp-based disordered  $A3$  structure [11, 12]. Ru is also expected to stabilize the hcp-based structure for CoPt films. In the present study, a CoPt film is prepared on an Ru underlayer hetero-epitaxially grown on MgO(111) substrate at 300 °C. A CoPt film is also formed directly on an MgO substrate. The detailed film structure and the magnetic property are investigated.

## 2 Experimental procedure

Thin films were deposited on polished MgO(111) substrates at 300 °C by using a radio-frequency (RF) magnetron sputtering system equipped with a reflection high-energy electron diffraction (RHEED) facility. The base pressures were lower than  $4 \times 10^{-7}$  Pa. Substrates were heated at 600 °C for 1 h in the chamber before film formation to obtain clean surfaces. Figures 2(a) and 3(a) show the RHEED pattern and the atomic force microscopy (AFM) image observed for a substrate after heating, respectively. The RHEED pattern exhibits a *Kikuchi* pattern, indicating that the surface is clean and smooth. The arithmetical mean surface roughness ( $R_a$ ) is estimated from the AFM image to be 0.2 nm.

$\text{Co}_{50}\text{Pt}_{50}$  (at. %) alloy and Ru targets of 3 in diameter were employed. The Ar gas pressure and the distance between target and substrate were kept constant at 0.67 Pa and 150 mm, respectively. The RF powers for  $\text{Co}_{50}\text{Pt}_{50}$  and Ru targets were respectively fixed at 45 and 60 W, where the deposition rate was 0.02 nm/s for both materials. A 10-nm-thick Ru underlayer and a 40-nm-thick CoPt film were sequentially deposited on the substrate. Figures 2(b) and 3(b) show the RHEED pattern and the AFM image observed for an Ru underlayer deposited on MgO substrate. A clear diffraction pattern corresponding to  $A3(0001)$  texture is recognized. An

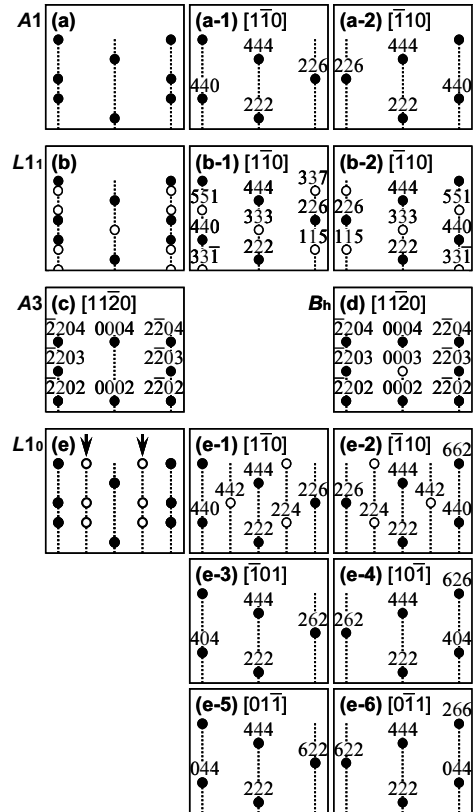


**Fig. 4.** Schematic diagrams of RHEED patterns simulated for (a)  $A1(111)$ , (b)  $L1_1(111)$ , (c)  $A3(0001)$ , (d)  $B_h(0001)$ , and (e)  $L1_0(111)$  surfaces. The incident electron beam is parallel to (a-1, b-1, e-1)  $[1\bar{1}0]$ , (a-2, b-2, e-2)  $[\bar{1}10]$ , (e-3)  $[\bar{1}01]$ , (e-4)  $[10\bar{1}]$ , (e-5)  $[01\bar{1}]$ , (e-6)  $[0\bar{1}1]$ , or (c, d)  $[11\bar{2}0]$ . The filled and open circles correspond to the fundamental and superlattice reflections, respectively.

Ru(0001) single-crystal underlayer is formed. The epitaxial orientation relationship is determined by RHEED as

$$\text{Ru}(0001)[11\bar{2}0] \parallel \text{MgO}(111)[1\bar{1}0].$$

The  $R_a$  value is 0.5 nm. A CoPt film of 40 nm thickness was also deposited directly on the substrate. The CoPt film compositions were confirmed by energy dispersive X-ray spectroscopy and the errors were less than 4 at. % from the target composition.

The surface structure was observed by RHEED and the epitaxial orientation relationship was determined. The resulting film structure was investigated by  $2\theta/\omega$ -scan out-of-plane,  $2\theta/\varphi$ -scan in-plane, and  $\beta$ -scan pole-figure X-ray diffractions (XRDs) with Cu-K $\alpha$  radiation ( $\lambda = 0.15418$  nm). The cross-sectional microstructure was observed by transmission electron microscopy (TEM). The TEM sample was first thinned mechanically and then ion-milled to be transparent for the electron beam accelerated at 300 kV. The magnetization curves were measured by using a vibrating sample magnetometer.

## 3 Results and discussion

Figures 2(c) and (d) show the RHEED patterns observed for CoPt films deposited on MgO(111) substrate and Ru(0001) underlayer, respectively. Clear patterns involving streaks are observed for both films. The RHEED patterns correspond to formations of  $A1(111)$ ,

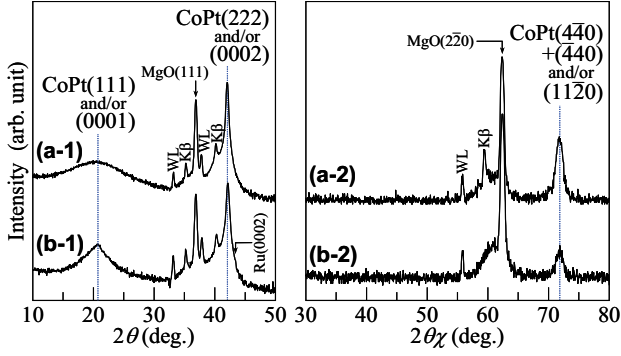


**Fig. 5.** (a-1, b-1) Out-of-plane and (a-2, b-2) in-plane XRD patterns of CoPt films deposited on (a) MgO substrate and (b) Ru underlayer. The scattering vector is parallel to (a-1, b-1) MgO[111] or (a-2, b-2) MgO[1 $\bar{1}$ 0]. The intensity is shown in a logarithmic scale. The small reflections noted as K $\beta$  and WL are due to Cu-K $\beta$  and W-L $\alpha$  radiations included in the X-ray source, respectively.

$L1_1(111)$ ,  $A3(0001)$ , and/or  $B_h(0001)$  crystals [figures 4(a)–(d)] and do not correspond to a diffraction pattern from  $L1_0(111)$  surface since the streaks shown by the arrows in figure 4(e) are absent. When streaks are included in an RHEED pattern, assignment of crystal structure from a group of  $A1$ ,  $L1_1$ ,  $A3$ , and  $B_h$  is not easy because the RHEED patterns are very similar as shown in figures 4(a)–(d). The structure is thus determined by XRD described later. The epitaxial orientation relationships are estimated by RHEED as follows,

$$\{A1 \text{ or } L1_1\}\text{-CoPt}(111)[1\bar{1}0], (111)[\bar{1}10] \\ \parallel \text{MgO}(111)[1\bar{1}0] \text{ or Ru}(0001)[11\bar{2}0],$$

$$\{A3 \text{ or } B_h\}\text{-CoPt}(0001)[1\bar{1}20] \\ \parallel \text{MgO}(111)[1\bar{1}0] \text{ or Ru}(0001)[11\bar{2}0].$$

CoPt epitaxial films with the close-packed plane parallel to the substrate surface are obtained. The  $A1$  and the  $L1_1$  crystals consist of two (111) variants whose atomic stacking sequences of close-packed plane are ABCABC.. and ACBACB... On the contrary, the  $A3$  and the  $B_h$  crystals with the sequence of ABAB... are single-crystals.

Figures 5(a-1) and (b-1) show the out-of-plane XRD patterns of CoPt films deposited on MgO(111) substrate and Ru(0001) underlayer, respectively. CoPt(111) and/or CoPt(0001) superlattice reflections are recognized in addition to CoPt(222) and/or CoPt(0002) fundamental reflections for both films, indicating that  $L1_1$  and/or  $B_h$  phases are involved. The  $S$  value can be estimated by comparing the intensities ( $I$ ) of fundamental and superlattice reflections.  $I$  is proportional to structure ( $F$ ), Lorentz-polarization ( $L$ ), and absorption ( $A$ ) factors [13]. In the present paper, an influence of temperature factor, which is often omitted when comparing intensities of two reflections, is not considered. The intensity ratio of superlattice to fundamental reflection is expressed as

$$I_s/I_f = (F_s F_s^* L_s A_s) / (F_f F_f^* L_f A_f), \quad (1)$$

where the subscripts of s and f refer to the superlattice and fundamental reflections, respectively. The  $F$  values of  $L1_1(111)$ ,  $L1_1(222)$ ,  $B_h(0001)$ , and  $B_h(0002)$  [7, 8] are respectively calculated to be  $16S(f_{Co}-f_{Pt})$ ,  $16(f_{Co}+f_{Pt})$ ,  $6S(f_{Co}-f_{Pt})$ , and  $6(f_{Co}+f_{Pt})$ , where  $f$  is the atomic scattering factor of Co or Pt. Therefore,  $S$  is expressed as

$$S = [(I_s/I_f) \{ (f_{Co}+f_{Pt})^2 (L_f A_f) \} / \{ (f_{Co}-f_{Pt})^2 (L_s A_s) \}]^{1/2} \quad (2)$$

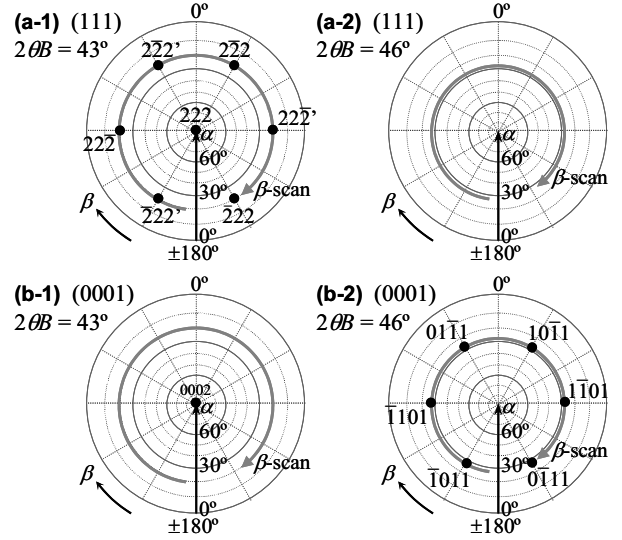


**Fig. 7.** Schematic diagrams of pole-figure XRD patterns of a CoPt film (a) with (111) orientation of  $A1$  and/or  $L1_1$  or (b) with (0001) orientation of  $A3$  and/or  $B_h$  epitaxially grown on MgO(111) substrate or Ru(0001) underlayer. The diffraction angle of  $2\theta B$  is fixed at (a-1, b-1)  $43^\circ$  or (a-2, b-2)  $46^\circ$ .

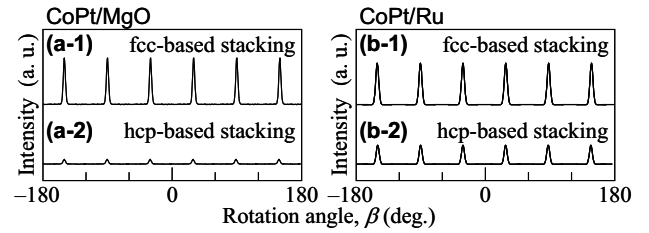


**Fig. 8.** Pole-figure XRD patterns of CoPt films deposited on (a) MgO substrate and (b) Ru underlayer measured by fixing the ( $\alpha$ ,  $2\theta B$ ) at (a-1, b-1) ( $20^\circ$ ,  $42^\circ$ ) and (a-2, b-2) ( $28^\circ$ ,  $45^\circ$ ), respectively. The intensity is shown in a linear scale.

for both crystal structures. The  $S$  values of films grown on MgO substrate and Ru underlayer are calculated to be 0.30 and 0.34, respectively. Similar  $S$  values are observed for both films. Figures 5(a-2) and (b-2) show the in-plane XRD patterns measured by making the scattering vector parallel to MgO[1 $\bar{1}$ 0]. CoPt(440)+(440) and/or CoPt(11 $\bar{2}$ 0) fundamental reflections are observed. No superlattice reflections corresponding to formation of  $L1_0$ -CoPt crystal are recognized, which are expected to appear around  $2\theta\chi = 33^\circ$ . The result agrees with the RHEED result.

In order to investigate the atomic stacking sequence of close-packed plane, pole-figure XRD was performed. Figure 7 shows the schematic diagrams of pole-figure XRD patterns of CoPt film with (111) orientation of  $A1$  and/or  $L1_1$  or with (0001) orientation of  $A3$  and/or  $B_h$  epitaxially grown on MgO(111) substrate or Ru(0001) underlayer. When the rotation angle of  $\beta$  is scanned by fixing the tilt and diffraction angles of ( $\alpha$ ,  $2\theta B$ ) at ( $20^\circ$ ,  $43^\circ$ ), six {222} reflections which originate from two variants of  $A1$  and/or  $L1_1$  with three-fold symmetry with respect to the perpendicular direction are recognized with  $60^\circ$  separation for a (111) film [figure 7(a-1)], whereas no reflections are observed for a (0001) film [figure 7(b-1)]. On the contrary, in the  $\beta$ -scan pattern measured by fixing the ( $\alpha$ ,  $2\theta B$ ) at ( $28^\circ$ ,  $46^\circ$ ), {1101} reflections of six-fold symmetry appear for a (0001) film [figure 7(b-2)], while

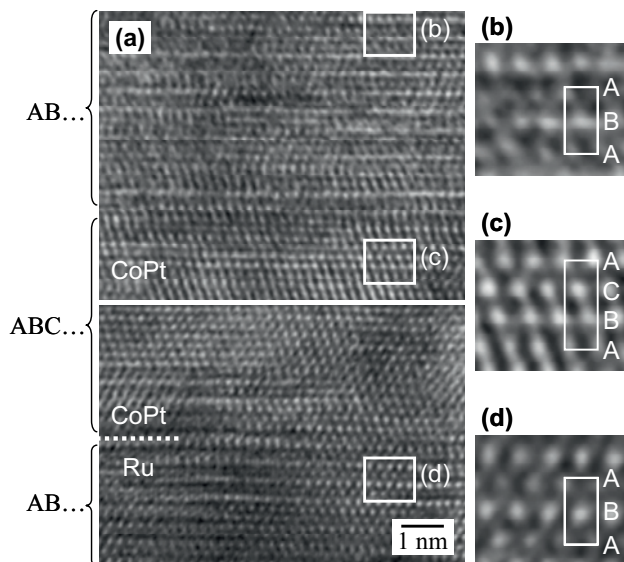


**Fig. 9.** (a) Cross-sectional TEM image observed for a CoPt film deposited on Ru underlayer. (b)–(d) Enlarged views of the areas surrounded by white square lines in (a).

no reflections are recognized for a (111) film [figure 7(a-2)]. Thus, the combination of two kinds of  $\beta$ -scan XRD reveals the atomic stacking sequence.

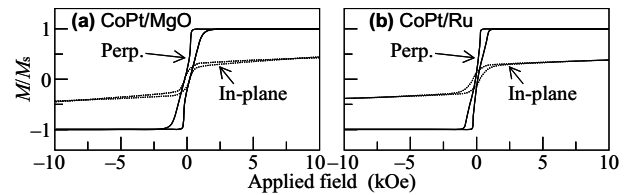
Figures 8(a-1) and (a-2) show the  $\beta$ -scan XRD patterns of CoPt film deposited on MgO substrate measured by fixing the ( $\alpha$ ,  $2\theta B$ ) at ( $20^\circ$ ,  $43^\circ$ ) and ( $28^\circ$ ,  $46^\circ$ ), respectively. Strong six reflections are observed in the pattern of figure 8(a-1), whereas very weak reflections are recognized in the pattern of figure 8(a-2). The result shows that the stacking sequence is ABCABC...+ACBACB... involving small amounts of stacking faults. fcc-based  $L1_1$  ordered phase is thus formed in the CoPt film deposited on MgO substrate.

Figure 8(b) shows the  $\beta$ -scan patterns of CoPt film deposited on Ru underlayer. Reflections are observed in both patterns. Therefore, the film consists of a mixture of ABCABC...+ACBACB... and ABAB... stacking sequences. hcp-based  $B_h$  phase is included in the film in addition to  $L1_1$  phase. The hcp-based stacking sequence is apparently promoted on the Ru underlayer. Figure 9(a) shows the cross-sectional high-resolution TEM image observed for the CoPt film grown on Ru underlayer. An atomically sharp boundary is recognized between the film and the underlayer. CoPt crystals with fcc- and hcp-based stacking sequences are apparently coexisting in the film [figures 9(b, c)].

Figures 3(c) and (d) show the AFM images observed for CoPt films deposited on MgO substrate and Ru underlayer, respectively. Flat surfaces are realized. The  $R_a$  values are 0.2 nm for both films. Figure 10 shows the magnetization curves. These films show strong perpendicular magnetic anisotropies. The magnetic properties are reflecting the magnetocrystalline anisotropies of ordered crystals of  $L1_1$  and/or  $B_h$ .

## 4 Conclusion

CoPt epitaxial films with the close-packed plane parallel to the substrate surface are prepared on an MgO(111) substrate and an Ru(0001) underlayer at 300 °C. The film formed on MgO substrate consists of fcc-based atomic



**Fig. 10.** Magnetization curves measured for CoPt films deposited on (a) MgO substrate and (b) Ru underlayer.

stacking sequence of close-packed plane along the perpendicular direction, whereas the film formed on Ru underlayer involves hcp-based stacking sequence in addition to fcc-based sequence. The order degrees of CoPt films deposited on MgO substrate and Ru underlayer are respectively 0.30 and 0.34. By considering the stacking sequence and the order degree, the crystal structures of CoPt films deposited on MgO substrate and Ru underlayer are determined to be  $L1_1$  and  $L1_1+B_h$ . Flat surfaces with the  $R_a$  value of 0.2 nm are realized for both films. The films show strong perpendicular magnetic anisotropies reflecting the magnetocrystalline anisotropies of  $L1_1$  and/or  $B_h$  phases. A CoPt alloy film with metastable ordered phase is useful as a high  $K_u$  magnetic material which can be applicable to future magnetic thin film devices.

## Acknowledgements

A part of this work was supported by JSPS KAKENHI Grant Number 25420294, JST A-STEP Grant Number AS242Z00169M, and Chuo University Grant for Special Research.

## References

1. Y. S. Shur, L. M. Magat, G. V. Ivanova, A. I. Mitsek, A. S. Yermolenko, O. A. Ivanov, *Fiz. Met. Metalloved.* **26**, 241 (1968).
2. O. A. Ivanov, L. V. Solina, V. A. Demshina, L. M. Magat, *Fiz. Metal. Metalloved.* **35**, 81 (1973)
3. M. Ohtake, S. Ouchi, F. Kirino, M. Futamoto, *J. Appl. Phys.* **111**, 07A708 (2012)
4. S. Iwata, T. Kato, S. Tsunashima, *IEEE Trans. Magn.* **33**, 3670 (1997)
5. H. Sato, T. Shimatsu, Y. Okazaki, H. Muraoka, H. Aoi, S. Okamoto, O. Kitakami, *J. Appl. Phys.* **103**, 07E114 (2008)
6. A. -C. Sun, F. -T. Yuan, J. -H. Hsu, H. Y. Lee, *Scripta Mater.* **61**, 713 (2009).
7. M. Ohtake, S. Ouchi, F. Kirino, M. Futamoto, *IEEE Trans. Magn.* **48**, 3595 (2012)
8. D. Suzuki, M. Ohtake, S. Ouchi, F. Kirino, M. Futamoto, *J. Magn. Soc. Jpn.* **36**, 336 (2012)
9. S. S. A. Razee, J. B. Staunton, B. Ginatempo, F. J. Pinski, E. Bruno, *Phys. Rev. Lett.* **82**, 5369 (1999)
10. G. R. Harp, D. Weller, T. A. Rabedeau, R. F. C. Farrow, M. F. Toney, *Phys. Rev. Lett.* **71**, 2493 (1993)
11. M. Takahashi, S. Saito, *J. Magn. Magn. Mater.* **320**, 2868 (2008)
12. K. M. Krishnan, T. Takeuchi, Y. Hirayama, M. Futamoto, *IEEE Trans. Magn.* **30**, 5115 (1994)
13. B. D. Cullity, *Elements of X-Ray Diffraction* (Addison-Wesley, Massachusetts, 1956)